Journal of Ultrafine Grained and Nanostructured Materials
https://jufgnsm.ut.ac.ir
Vol. 56, No.2, December 2023, pp. 194-204
Print ISSN: 2423-6845 Online ISSN: 2423-6837
DOI: 10.22059/jufgnsm.2023.02.08

Effects of annealing treatment on microstructure, tensile properties and electrical conductivity of copper-graphene nanocomposite fabricated by accumulative roll bonding

Ali Reza Eivani[1,*], Hamid Reza Jafarian[1], Ali Shojaei[1]

[1]School of Metallurgy and materials Engineering, Iran University of Science and Technology, Tehran, Iran.

Recieved: 26 Octobor 2023; Accepted: 16 December 2023

**Corresponding author email: aeivani@iust.ac.ir*

ABSTRACT

In this article, effects of annealing treatment on the evolution of microstructure, tensile properties and electrical resistivity of copper-graphene nanocomposites are investigated. In order to fabricate the nanocomposite, graphene nanopowder was ball-milled after being mixed with copper powder to form a mixture of copper-graphene powder (CuG). Hot rolled copper sheets were used as the matrix of the composite which were annealed prior to accumulative roll bonding (ARB). The nanocomposite was fabricated using 2, 4 and 6 cycles of ARB leading to 20, 40 and 160 multi-layered nanocomposites. Despite increased mechanical strength, the elongation to failure and the electrical conductivity were significantly reduced which were attributed to the high defect density after severe cold deformation and strength-ductility trade-off. The effect of cold deformation on increasing electrical resistivity was so significant that no positive effects of addition of 1% CuG on reducing resistivity was observed but a slight improvement was found in the sample with 2% CuG. However, after annealing at 500 C for 2 h, ductility was fully recovered to the initial value and the electrical resistivity was significantly reduced in the nanocomposite. This was attributed to the fact that a fully recrystallized grain structure was achieved after annealing. Percentage of reinforcing agent and the thickness of the stacking layers were found to determine the final grain size. Electrical conductivity of the nanocomposite was found to significantly improve with annealing. Indeed, the electrical conductivity of the annealed 6ARB-2%CuG composite was higher than the initially annealed copper sheet while the strength and ductility were increased, as well. This determines that the combination of ARB and annealing can be used as an effective method for fabrication of copper-graphene nanocomposites.

Keywords: Composite; Conductivity; Copper; Graphene; Rolling.

1. Introduction

Copper is a highly conductive material with acceptable level of strength, ductility and formability. Therefore, it is widely used in industry where reduced production costs in addition to high conductivity are required. Indeed, electrical copper is mostly used in the form of rolled sheets at fully annealed condition, i.e., recrystallized grain structure with minimum defect density, which is likely to show the highest conductivity [1,2]. Due to its superior value, increasing electrical conductivity of copper is not an easy job. Such high electrical conductivity of copper would be easily degraded instead of being improved by changing processing conditions. For example, cold deformation has been found to significantly degrade electrical conductivity of copper due to imposing a high density of defects including, vacancies, dislocations and

grain boundaries [3].

Fabrication of composites and nanocomposites is found to be an effective method to acquire products with simultaneously improved physical and mechanical properties [4–6]. For example, mechanical strength [7–9], wear [10,11] and fatigue and corrosion resistance [12] and few other properties have been found to improve in different metallic or non-metallic materials. Composite fabrication approach is mostly based on the hypothesis to combine and benefit different positive effects of additives and matrices [4–8]. For example, in metal matrix composites (MMCs) the metallic matrix provides the ductility and/or toughness while reinforcing particles or fibers provide wear resistance and hardness [4–8]. Therefore, it seems to be possible to fabricate a copper based MMC with simultaneously improved mechanical properties and electrical conductivity.

Copper-based MMCs have been previously fabricated by different methods and approaches [13–24] with various additives [25–29]. However, no considerable improvement in strength has been achieved with negligible achievement in improving conductivity. Among different methods, solid state deformation may be a unique processing method due to the high deformability of copper in addition to the fact that it may result in an optimum distribution of reinforcing particles [13–22] which is a vital parameter to achieve the maximum out of a composite structure. It should be noted that electrical conductivity is likely to be degraded during deformation because it results in enhanced crystal defects [30–33].

In a previous attempt to fabricate copper-based nanocomposite, slight improvement in electrical conductivity was only achieved by addition of 2 wt.% CuG and application of 6 cycles of ARB while the ductility was reduced to half of its initial value. Both parameters, i.e., conductivity and ductility, may be possible to be improved by application of annealing treatment. In the current article, effects of post-fabrication annealing treatment on the evolution of microstructure, tensile properties and electrical conductivity of ARB-fabricated Cu-CuG nanocomposites are investigated. It is supposed that with annealing, the defects and dislocations density reduce and reach to its initial numbers in the annealed pure copper sheets. Therefore, variations in microstructure and tensile properties are expected in addition to changes in electrical resistivity.

2. Experimental procedure

Hot rolled sheets of electrical copper were received with 0.5 mm thickness and chemical composition shown in Table 1. In order to remove effects of previous deformation, the plates were fully annealed at 500 °C for 2 h and cooled in the furnace. Prior to rolling, the sheets were cut into 150 by 150 mm plates, cleaned, washed and degreased by acetone followed by brushing using 0.3 mm thick steel brush. 5 layers of the plates were prepared to be stacked on each other prior to rolling.

Multilayer graphene powder with an average thickness of 10 nm was used as additive to fabricate copper-graphene nanocomposite. For preparation of the graphene additive, 0.2 g graphene was mixed with 9.8 g copper powder in ethanol and dried in air to achieve a mixture of copper and graphene (CuG). The CuG powder was milled in a H13 tool steel cup and balls for 4 h at 400 rpm. The diameter of the balls was 10 mm and the weight ratio of balls to CuG powder was 15:1.

Accumulative roll bonding (ARB) was used to fabricate copper-graphene nanocomposites. For this purpose, 1 and 2 g of CuG powder were added onto the plate. The assembly was rolled for 50 % using a 50-ton rolling stand having mills with 170 mm diameter and 200 mm width, resulting in a sandwich of Cu and CuG. The resulting sandwich was ARB rolled for 2, 4 and 6 cycles and a multilayer Cu-CuG nanocomposite was fabricated with 10, 40 and 160 layers but a similar percentage of CuG powder. The samples were annealed at 500 °C for 2 h in salt bath. After annealing, the samples were cooled down to 100 °C in the salt bath, continued by air cooling to room temperature.

Huvitz optical microscope was used to inves-

Table 1- Chemical composition of the alloy used in this investigation

Element	Cu	Ag	Si	P	Sn	Pb	Co	Ni	Fe	Zn
Wt. %	Balance	0.006	<0.005	<0.005	<0.01	<0.01	0.01	0.01	0.01	0.02

tigate the microstructures of the fabricated nanocomposites. The cross sections chosen for the microstructure observation were in RD-ND direction. The etchant used for this purpose was a solution of 1 g $FeCl_3$, 10 ml HCl and 10 ml distilled water. The samples were etched for 5 sec in the solution after grinding and polishing. Hondsfield H50Ks tensile testing machine was used for evaluation of mechanical properties of the composite. The tests were conducted at 0.1 mm/sec according to ASTM E8 standard. The length, width and thickness of the specimens were 10, 2.5 and 1 mm, respectively. Fracture surfaces were investigated using Tescan VEGA/XMU SEM microscope. Electrical resistivity of the samples was measured using MICROHMMETER CA 6250 equipped with a two points probe.

3. Results and discussion

3.1. Constituents of the composite

3.1.1. Graphene powder

SEM, X-ray diffraction pattern and Raman spectrum of the powder prior to mixing are shown in Figure 1. It is clear that graphene has a laminar structure. The layer's thickness of this powder has been previously measured and fall into the range of less than 10 nm [34]. In the XRD pattern, a single peak related to the (002) plane of graphene is detected. Raman spectrum indicates that the intensity of the 2D and G peaks are 4720 and 3657.

3.1.2. Copper powder

The size and morphology of the copper powder prior to milling is shown in Figure 2 (a). The initial average size of the copper powder is around 5 μm. It can be seen in Figure 2 (b) that after mixing with graphene and milling (to produce CuG powder), the average size of the particles increases to 12 μm. This size increase is attributed to coarsening of the particles during milling. This is indeed because of the high ductility of copper which flatten and increase in size instead of fragmentation and size reduction. XRD pattern and EDS spectrum of the prepared CuG powder are shown in Figure 2 (c) and (d). A single copper phase is detected during XRD. Graphene is not detected which is due to its low weight percentage, which falls beyond the detection limit of XRD. In addition, graphene is not detected by EDS, as carbon is an element which is too difficult to be detected. The absence of iron is extremely important since trace impurities can significantly degrade the electrical conductivity of copper [35,36].

3.1.3. Copper sheets

The initial microstructures of the copper sheets after full annealing and prior to ARB processing are shown in Figure 3. The grain structure is fully recrystallized and the microstructure is composed of fine and equi-axed grain structure in addition to a few numbers of annealing twins. Average grains size of the sample was measured according to ASTM E112 standard to be around 27 μm.

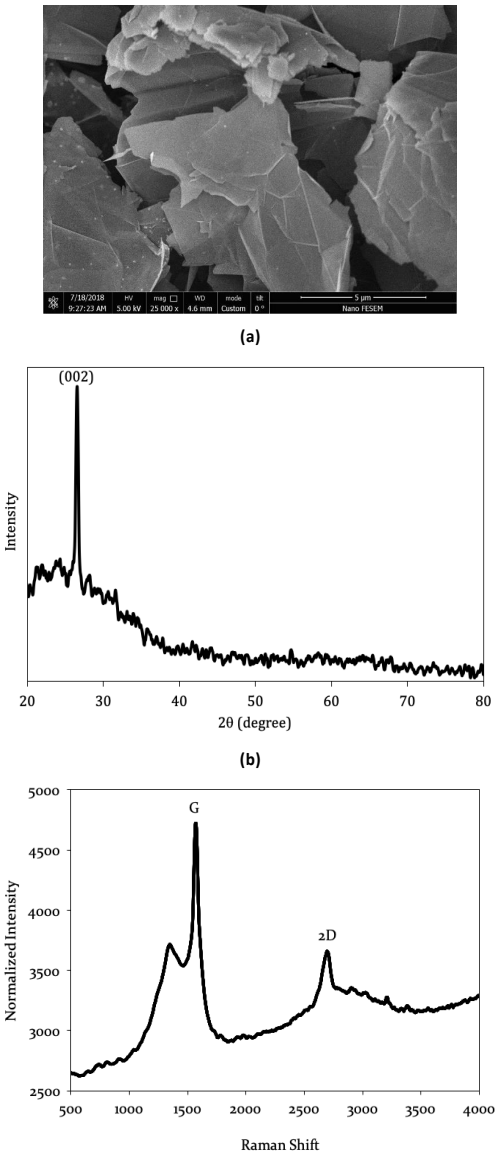

Fig. 1- Results of (a) SEM, (b) XRD and (c) Raman spectrum of the initial graphene nanopowder prior to milling.

3.2. As-fabricated nanocomposite

Tensile stress-strain curves of the as-fabricated nanocomposites with 2, 4 and 6 cycles of ARB in comparison with that for the initial copper sheet are shown in Figure 4. The values of yield strength (YS), ultimate tensile strength (UTS) uniform elongation (eu) and elongation to failure (ef) of each sample is extracted and presented in Table 2 and a comparison between the extracted data is presented in Figure 5. It can be seen that with application of 2 cycles of ARB, the strength is significantly increased and the ductility is reduced. Indeed, YS and UTS increase from 49 and 204.2 MPa to 255 and 420.1 MPa. However, the uniform elongation (eu) and elongation to failure (ef) reduce from 43.6 and 48.9 % to 3.3 and 8.4 %, respectively. The enhancement in strength can be attributed to an increase in dislocation density which causes significant work hardening and increased strength [37]. Due to the significant work hardening caused by severe plastic deformation (SPD) during ARB, there is not more room for plastic deformation during tensile testing. Therefore, the samples break shortly after they yield. Indeed, the tensile test sample starts to deform locally, leading to necking, and final fracture. Such deformation behavior of the material would clearly affect the ductility in terms of reduced eu and ef. Indeed, the capacity of the fabricated nanocomposite to withstand deformation during tensile testing is significantly reduced and the sample enters the

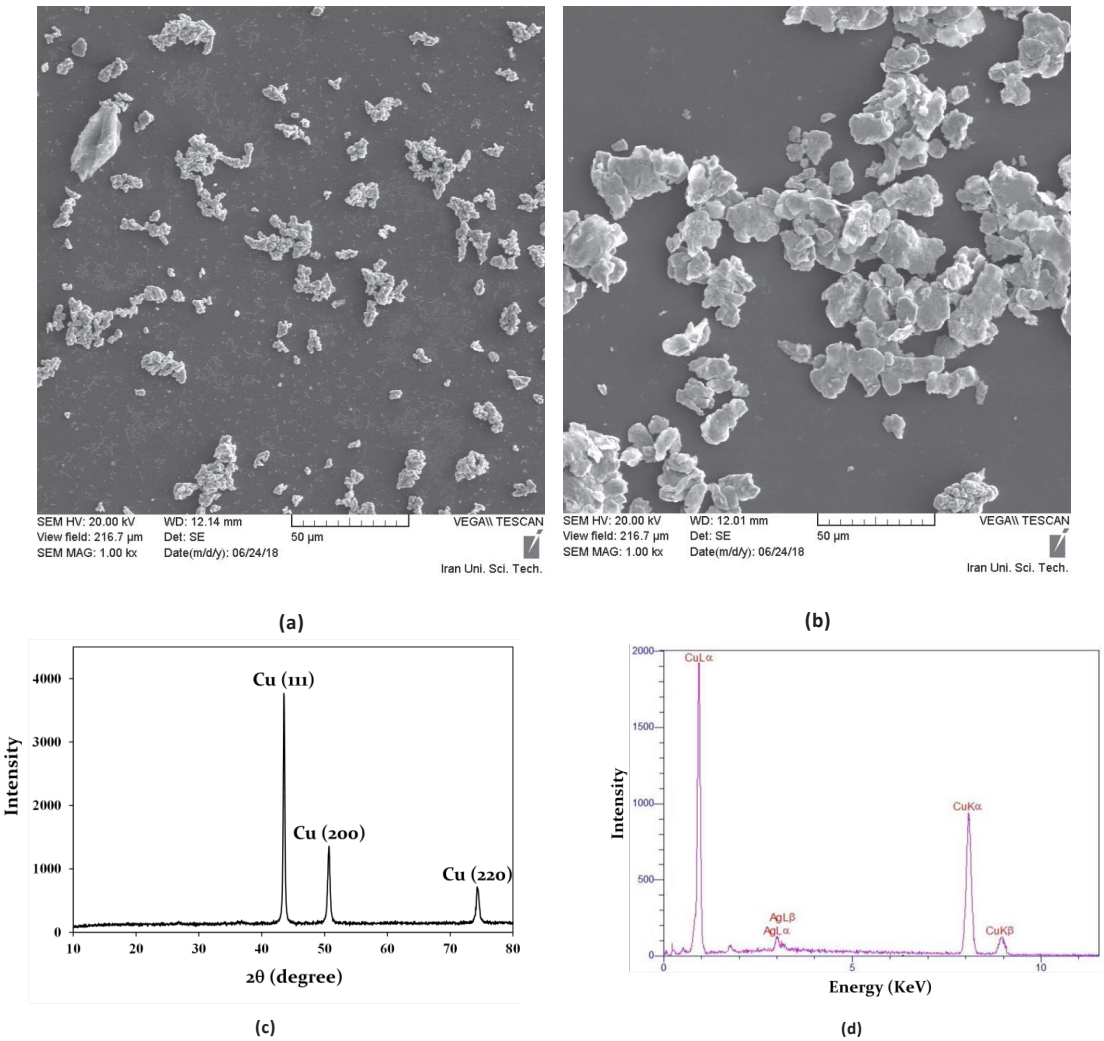

Fig. 2- (a) SEM image of copper powder prior to mixing and milling, (b) SEM image, (c) XRD pattern and (d) EDS spectrum of the mixed CuG powder after milling.

localized deformation zone rapidly which results in limited eu. Eventually, the negligible localized deformation might be attributed to the occurrence of delamination of the stacking layers of the nanocomposite, as observed in Figure 6. The fracture surface of the tensile test samples at higher magnification which is shown, in the case of 1%CuG-4ARB nanocomposite, in Figure 7 consists of few stackings but separated layers (delaminated layers) of copper which indicates debonding of multiple layers during tensile test. Observed delamination may have been initiated from voids (see Figure 8) and/or debonding of the CuG particle from the matrix. The presence of the voids can be related to an unacceptable or poor bonding quality between successive stacking layers of the nanocomposites [37]. It can be seen in Figure 8 that the void density and size reduce with increasing ARB cycles. This results in a more solid bonding and consequently further resistance of the composite to delamination. The net result of improved bonding quality can be observed in terms of enhanced localized deformation and increased difference between eu to ef. However, the strength is not significantly increased with further deformation, e.g., not a significant difference between 1%CuG-4ARB and 1%CuG-6ARB nanocomposites. This may be attributed to the fact that the work hardenability of copper becomes saturated with a level of SPD deformation. Previous investigations show that the required level of deformation to reach saturation is around an equivalent strain of 2 [38] which is known to be the case after 2 or more cycles of ARB.

In the 2%CuG-6ARB nanocomposite which is fabricated by addition of 2% of CuG, further voids are observed in comparison with 1%CuG-6ARB. In addition, higher fraction of CuG may result in increased debonding between the additives and the matrix which facilitates fracture initiation. Consequently, earlier fracture is expected during tensile testing which is also observed in Figure 4 (b). In addition, enhancement in YS and/or UTS can be hardly noticed in comparison to the sample with 1% CuG. Therefore, one can conclude that the graphene nanoparticles are not expected to have significant strengthening effects in the fabricated composite.

3.3. After annealing

Tensile stress-strain results on the nanocompos-

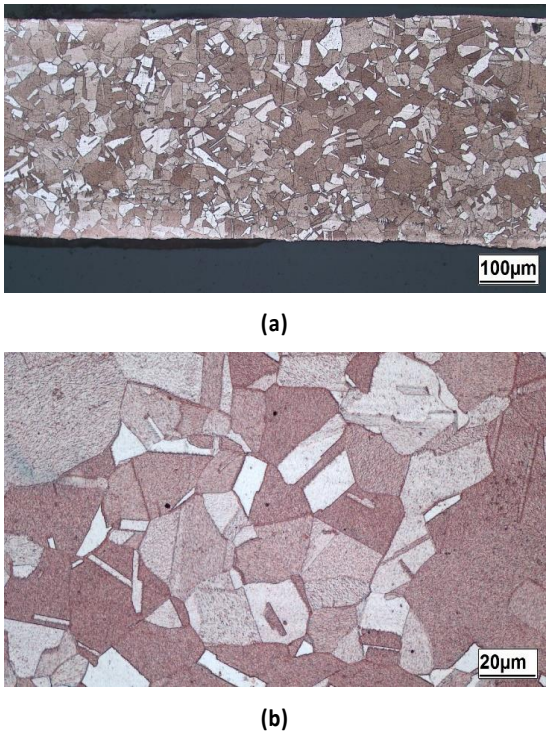

Fig. 3- Initial microstructure of the copper sheet after annealing at 500 °C for 2 h, at (a) low and (b) high magnification.

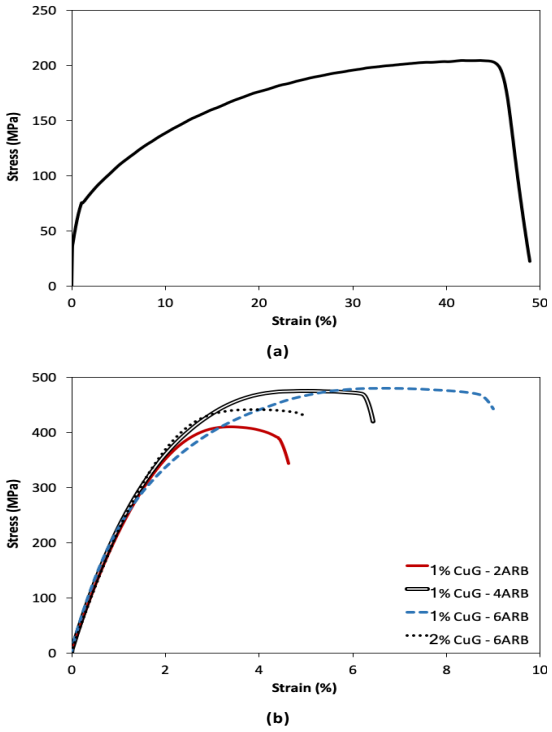

Fig. 4- Engineering tensile stress-strain curves of the (a) initially annealed copper sheet and (b)as- fabricated nanocomposite.

ite samples after annealing are shown in Figure 9. In comparison to the as-fabricated nanocomposite, the flow stress, YS and UTS reduce. For example, YS has reduced after annealing from 255, 262 and 270 to 60.5, 69.3 and 63.8 MPA in 1%CuG added nanocomposites fabricated with 2, 4 and 6 ARB cycles. This can be correlated to the effect of annealing on the microstructure of the nanocomposites which are shown in Figure 8. It can be seen that the microstructures are fully recrystallized and composed of fine equi-axed grains. Such recrystallized structure is reduced in internal energy and consequently, no share of work hardening and cold plastic deformation remains in the strength of the composite and eventually reduction in strength occurs.

After annealing, a slight improvement in the bonding quality can be observed as well. Indeed, in some areas the grains have grown into the adjacent layer forming a coarse grain and consequently, no sign of the interface remains. Yet in some other areas, the interface can be detected which may be an indication of no solid bonding between the layers. Such improvement in bonding quality may be a reason for improved tensile strength and ductility, as it results in reduced delamination during tensile test.

The microstructures of the nanocomposites after annealing are shown in Figure 10. It is also possible to see that the recrystallized grain structure is typically finer that that in the initially annealed sheet (see Figure 3). It is important to note that despite of reduction in the strength of the composite after annealing, the strength is still higher than the initially annealed sheets. This can be attributed to

Table 1- Extracted values of yield strength (YS), ultimate tensile strength (UTS) uniform elongation (eu) and elongation to failure (ef) of the nanocomposites

	YS (MPa)	UTS (MPa)	e_u (%)	e_f (%)
as-annealed	49.0	204.2	43.6	48.9
1%CuG-2ARB	255.0	420.1	3.3	8.4
1%CuG-4ARB	262.0	432.7	4.5	8.2
1%CuG-6ARB	270.0	466.9	5.3	9.8
2%CuG-6ARB	270	220.3	57.3	62.7
1%CuG-2ARB-ann	56.1	220.3	57.3	62.7
1%CuG-4ARB-ann	60.5	217.2	50.7	58.7
1%CuG-6ARB-ann	69.3	208.8	44.9	50.4
2%CuG-6ARB-ann	63.8	201.1	42.5	45.2

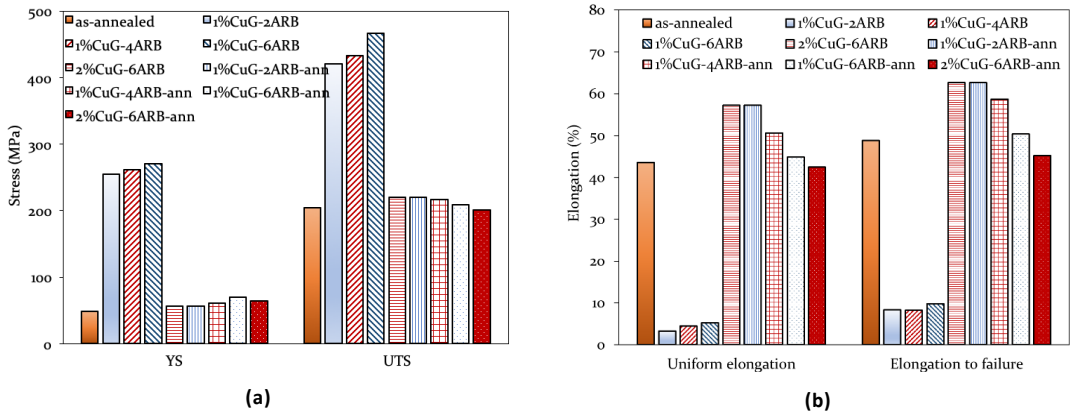

Fig. 5- A comparison between extracted tensile test data.

the finer grain structure and the interfaces which remain between the stacking layers which contribute in increasing the strength of the composite. In addition, one may note that the elongations of all annealed nanocomposites are more than the initially annealed copper sheet and reduces with higher ARB cycles. This may be attributed to the finer grain structure which is achieved in the annealed samples with higher cycles of ARB processing.

One can see in Figure 10 that the grain structure is finer in the case of the samples with higher number of stacking layers, i.e., further ARB cycles. This is despite the fact that all samples have gone through a full anneal treatment at 500 °C. Indeed, after such severe annealing treatment, all previous effects of deformation are likely to be removed and a grain structure with constant grain size would be achieved. Such constant grain size or limiting grain size is expected to be determined by the percentage of the particles with Zener pinning effects. CuG particles are likely to have such an effect. However, the difference between nanocomposites with similar levels of CuG, i.e., 1% in 2, 4 and 6 ARB can only be explained by reduction in the thickness of the stacking layers. One can see in the microstructures that no grain is observed to be grown trans-layer,

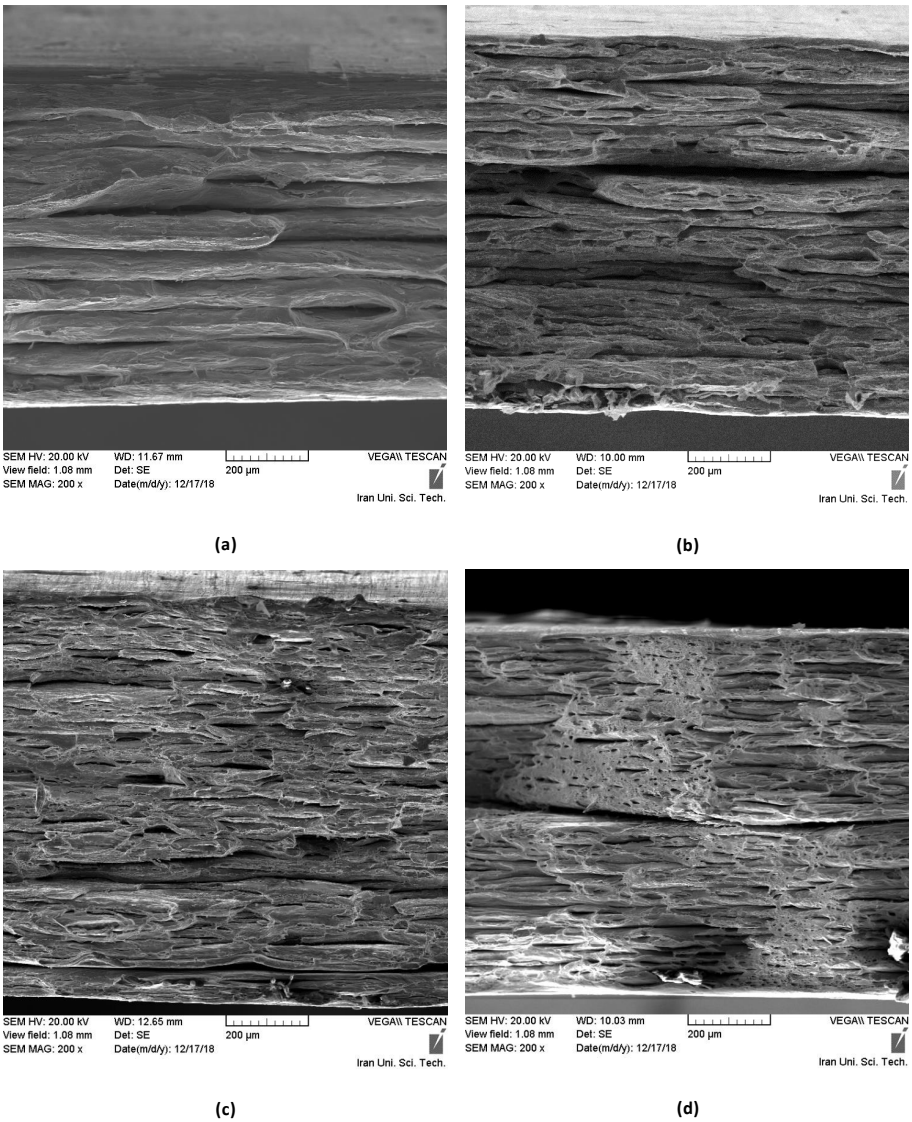

Fig. 6- SEM images showing the fracture surfaces of the nanocomposites, (a) 1%CuG-2ARB, (b) 1%CuG-4ARB, (c) 1%CuG-6ARB and (d) 2%CuG-6ARB.

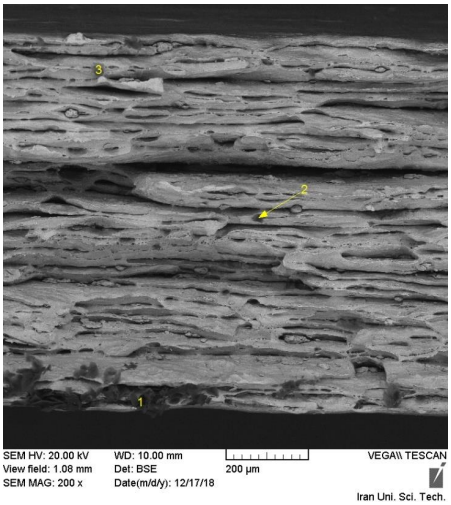

Fig. 7- Top-view SEM image of the fracture surface of the 1%CuG-4ARB nanocomposite showing delamination of the stacking layers of copper and debonding of the CuG particles from the matrix.

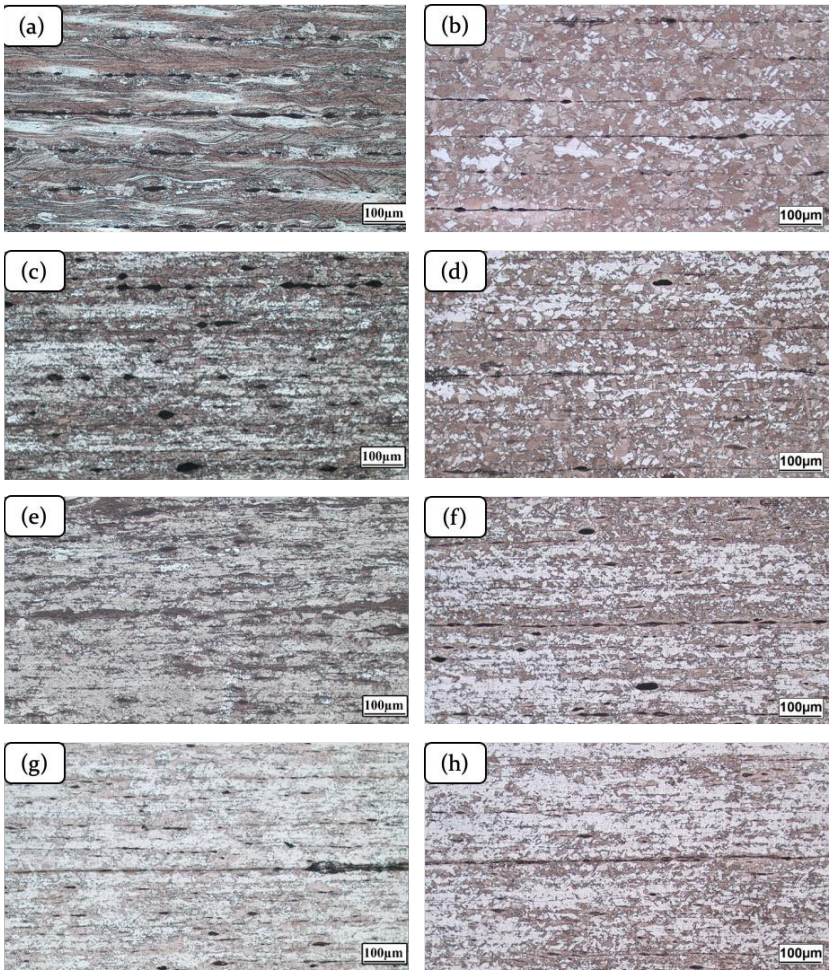

Fig. 8- Grain structure of the nanocomposites, (a) and (b) 1%CuG-2ARB, (c) and (d) 1%CuG-4ARB, (e) and (f) 1%CuG-6ARB and (g) and (h) 2%CuG-6ARB in as-fabricated (a), (c), (e) and (f) and after annealing (b), (d), (f) and (h).

i.e., passing from one sheet layer of the composite to the next. Such impossibility of trans-layer growth causes an artificial obstacle against grain growth. Therefore, the limiting grain size achieved in the nanocomposites with further ARB deformation are finer than those with less deformation. Despite the effects of the layers thickness, the percentage of CuG particles looks likely to have further effect on reduction in grain size, observed by finer grain size of 6ARB-2%CuG in comparison to 6ARB-1%CuG. Indeed, the interface between stacking layers of the copper sheets in the nanocomposites has limited the grain growth and has resulted in a finer grain structure. At higher level of reinforcing additions, i.e., 2% CuG, the minimum values of eu and ef are achieved which may, like before, be attributed to the occurrence of more delamination caused by the existing voids contributing in earlier fracture of the composite sample during tensile testing.

3.4. Electrical resistivity

It can be seen that in the samples which are fabricated by one and two cycles of ARB, the electrical resistivity is higher than the pure copper, even after annealing (Table 3). This is despite of the fact that optical microscopy indicated a fully annealed sample with recrystallized and equiaxed grain structure. Indeed, as graphene with high electrical conductivity is supposed to improve the electrical conductivity of the nanocomposite, one may conclude that the interface between stacking layers in the nanocomposite has resulted in an ineffective graphene addition on increased electrical conductivity. This may be attributed to the fact that an inappropriate bonding between the stacking plates has formed which result in reduced electrical conductivity. It can be seen that in the sample which is ARB processed for 6 cycles, this issue is solved and eventually reduced electrical conductivity is

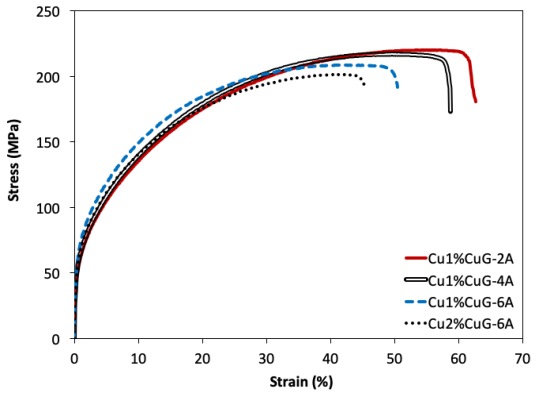

Fig. 9-Tensile stress-strain curves of the nanocomposite after annealing.

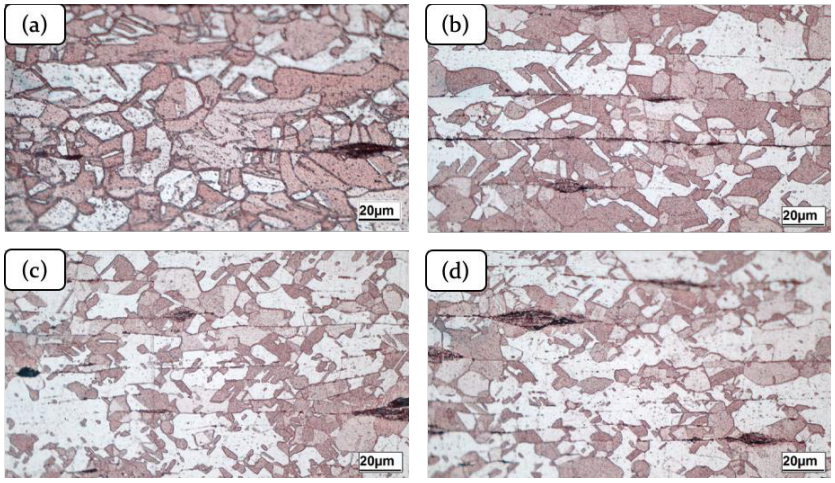

Fig. 10-Grain structure of the nanocomposites after annealing, (a) 1%CuG-2ARB, (b) 1%CuG-4ARB, (c) 1%CuG-6ARB and (d) 2%CuG-6ARB.

achieved. As mentioned before, comparison between the mechanical strength of this sample with the annealed copper sheet indicates that utilization of weak graphene additives has not resulted in reduced strength.

4. Conclusions

In this investigation, the effect on annealing treatment on the microstructure, tensile properties and electrical conductivity of the ARB-fabricated copper-based graphene reinforced nanocomposite is investigated. The study was aimed at improving the electrical conductivity of the nanocomposite with controlled loss of strength and re-achieving the initial ductility of copper sheets. According to the results of the current investigation, the following conclusions are made;

1) Yield strength (YS) and ultimate tensile strength (UTS) are found to significantly increase by 2 cycles of ARB processing while the elongation reduces. With further ARB processing, the strength is almost unchanged while ductility improves. This was attributed to the more significant delamination in the nanocomposites fabricated with smaller deformation, e.g., 2 cycles of ARB.

2) After annealing treatment, the elongation of the nanocomposite is recovered and reaches to values eventually slightly higher than the initial copper sheet.

3) Graphene is found to have no clear strengthening effect in the fabricated nanocomposite. This effect is neither obvious in as-fabricated nor annealed condition.

4) A fully recrystallized grain structure is achieved after annealing at 500 C for 2 h. However, the grain size is not similar for all fabricated nanocomposites. Indeed, two factors, i.e., the percentage of reinforcing agent and the thickness of the stacking layers, determine the final grain size.

5) Electrical conductivity of the nanocomposite is found to significantly improve with annealing. In addition, the electrical conductivity of the annealed 6ARB-2%CuG composite is higher than the initially annealed copper sheet while it has an increased strength and ductility. This determines that the combination of ARB and annealing can be used as an effective method for fabrication of copper-graphene nanocomposites.

5. Data availability

The raw data required to reproduce these findings are available upon request.

Table 3- Extracted values of yield strength (YS), ultimate tensile strength (UTS) uniform elongation (eu) and elongation to failure (ef) of the nanocomposites

Sample	Specific electrical resistivity
as-annealed	1.73
1% CuG - 2 ARB	1.89
1% CuG - 4 ARB	1.91
1% CuG - 6 ARB	1.77
2% CuG - 6 ARB	1.67
1% CuG - 2 ARB - ann	1.86
1% CuG - 4 ARB - ann	1.86
1% CuG - 6 ARB - ann	1.71
2% CuG - 6 ARB - ann	1.61

Refrences

1. Yabuki A, Arriffin N. Electrical conductivity of copper nanoparticle thin films annealed at low temperature. Thin Solid Films. 2010;518(23):7033-7.
2. Lim JW, Isshiki M. Electrical resistivity of Cu films deposited by ion beam deposition: Effects of grain size, impurities, and morphological defect. Journal of Applied Physics. 2006;99(9).
3. Abbas SF, Kim T-S. Effect of lattice strain on the electrical conductivity of rapidly solidified copper-iron metastable alloys. Journal of Alloys and Compounds. 2018;732:129-35.
4. Mortensen A, Llorca J. Metal Matrix Composites. Annual Review of Materials Research. 2010;40(1):243-70.

5. Casati R, Vedani M. Metal Matrix Composites Reinforced by Nano-Particles—A Review. Metals. 2014;4(1):65-83.
6. Ibrahim IA, Mohamed FA, Lavernia EJ. Particulate reinforced metal matrix composites — a review. Journal of Materials Science. 1991;26(5):1137-56.
7. Güler Ö, Bağcı N. A short review on mechanical properties of graphene reinforced metal matrix composites. Journal of Materials Research and Technology. 2020;9(3):6808-33.
8. Ramnath BV, Elanchezhian C, Annamalai RM, Aravind S, Atreya TS, Vignesh V, Subramanian C. Aluminium metal matrix composites–a review. Rev. Adv. Mater. Sci. 2014 Aug 1;38(5):55-60.
9. Tjong SC. Novel Nanoparticle-Reinforced Metal Matrix Composites with Enhanced Mechanical Properties. Advanced Engineering Materials. 2007;9(8):639-52.
10. Samal P, Vundavilli PR, Meher A, Mahapatra MM. Recent progress in aluminum metal matrix composites: A review on processing, mechanical and wear properties. Journal of Manufacturing Processes. 2020;59:131-52.
11. Reddy PV, Kumar GS, Krishnudu DM, Rao HR. Mechanical and Wear Performances of Aluminium-Based Metal Matrix Composites: A Review. Journal of Bio- and Tribo-Corrosion. 2020;6(3).
12. Eivani AR, Tabatabaei F, Khavandi AR, Tajabadi M, Mehdizade M, Jafarian HR, Zhou J. The effect of addition of hardystonite on the strength, ductility and corrosion resistance of WE43 magnesium alloy. Journal of Materials Research and Technology. 2021;13:1855-65..
13. Afifeh M, Hosseinipour SJ, Jamaati R. Nanostructured copper matrix composite with extraordinary strength and high electrical conductivity produced by asymmetric cryorolling. Materials Science and Engineering: A. 2019;763:138146.
14. Feng J, Liang S, Song K, Guo X, Zhang Y, Li G, Volinsky AA. Effects of Particle Characteristic Parameters on the Electrical Conductivity of TiB2/Cu Composites: A Modified Model for Predicting Their Electrical Conductivity. Journal of Materials Engineering and Performance. 2019;28(7):4316-23.
15. Zuo T, Li J, Gao Z, Wu Y, Zhang L, Da B, et al. Simultaneous improvement of electrical conductivity and mechanical property of Cr doped Cu/CNTs composites. Materials Today Communications. 2020;23:100907.
16. Saboori A, Pavese M, Badini C, Fino P. A Novel Approach to Enhance the Mechanical Strength and Electrical and Thermal Conductivity of Cu-GNP Nanocomposites. Metallurgical and Materials Transactions A. 2017;49(1):333-45.
17. Arnaud C, Lecouturier F, Mesguich D, Ferreira N, Chevallier G, Estournès C, et al. High strength – High conductivity double-walled carbon nanotube – Copper composite wires. Carbon. 2016;96:212-5.
18. Han B, Guo E, Xue X, Zhao Z, Li T, Xu Y, et al. Fabricating and strengthening the carbon nanotube/copper composite fibers with high strength and high electrical conductivity. Applied Surface Science. 2018;441:984-92.
19. Chen Y, Zhang X, Liu E, He C, Shi C, Li J, et al. Fabrication of in-situ grown graphene reinforced Cu matrix composites. Sci Rep. 2016;6:19363.
20. Dong L, Chen W, Zheng C, Deng N. Microstructure and properties characterization of tungsten–copper composite materials doped with graphene. Journal of Alloys and Compounds. 2017;695:1637-46.
21. Tardieu S, Mesguich D, Lonjon A, Lecouturier F, Ferreira N, Chevallier G, et al. Nanostructured 1% silver-copper composite wires with a high tensile strength and a high electrical conductivity. Materials Science and Engineering: A. 2019;761:138048.
22. Pan Y, Xiao S, Lu X, Zhou C, Li Y, Liu Z, et al. Fabrication, mechanical properties and electrical conductivity of Al_2O_3 reinforced Cu/CNTs composites. Journal of Alloys and Compounds. 2019;782:1015-23.
23. Çam G, Mistikoglu S. Recent Developments in Friction Stir Welding of Al-alloys. Journal of Materials Engineering and Performance. 2014;23(6):1936-53.
24. Heidarzadeh A, Mironov S, Kaibyshev R, Çam G, Simar A, Gerlich A, et al. Friction stir welding/processing of metals and alloys: A comprehensive review on microstructural evolution. Progress in Materials Science. 2021;117:100752.
25. Fathy A, Elkady O, Abu-Oqail A. Microstructure, mechanical and wear properties of Cu–ZrO_2 nanocomposites. Materials Science and Technology. 2017;33(17):2138-46.
26. Fathy A, Elkady O, Abu-Oqail A. Synthesis and characterization of Cu–ZrO_2 nanocomposite produced by thermochemical process. Journal of Alloys and Compounds. 2017;719:411-9.
27. Fathy A. Investigation on microstructure and properties of Cu-ZrO_2 nanocomposites synthesized by in situ processing. Materials Letters. 2018;213:95-9.
28. Fathy A, Elkady O, Abu-Oqail A. Production and properties of Cu-ZrO_2 nanocomposites. Journal of Composite Materials. 2017;52(11):1519-29.
29. Shehata F, Fathy A, Abdelhameed M, Moustafa SF. Preparation and properties of Al_2O_3 nanoparticle reinforced copper matrix composites by in situ processing. Materials & Design. 2009;30(7):2756-62.
30. Lu L, Shen Y, Chen X, Qian L, Lu K. Ultrahigh Strength and High Electrical Conductivity in Copper. Science. 2004;304(5669):422-6.
31. Uddin SM, Mahmud T, Wolf C, Glanz C, Kolaric I, Volkmer C, et al. Effect of size and shape of metal particles to improve hardness and electrical properties of carbon nanotube reinforced copper and copper alloy composites. Composites Science and Technology. 2010;70(16):2253-7.
32. Abbas SF, Seo S-J, Park K-T, Kim B-S, Kim T-S. Effect of grain size on the electrical conductivity of copper–iron alloys. Journal of Alloys and Compounds. 2017;720:8-16.
33. Abbas SF, Kim T-S. Effect of lattice strain on the electrical conductivity of rapidly solidified copper-iron metastable alloys. Journal of Alloys and Compounds. 2018;732:129-35.
34. Eivani AR, Shojaei A, Park N, Jafarian HR. Fabrication of Cu-CuG nanocomposites with enhanced mechanical strength and reduced electrical resistivity. Journal of Materials Research and Technology. 2021;11:650-66.
35. Addicks L. The Electrical Conductivity of Commercial Copper. Transactions of the American Institute of Electrical Engineers. 1903;XXII:695-702.
36. Heuer RP. THE EFFECT OF IRON AND OXYGEN ON THE ELECTRICAL CONDUCTIVITY OF COPPER. J Am Chem Soc. 1927;49(11):2711-20.
37. Eivani AR, Shojaei A, Salehi MT, Jafarian HR, Park N. On the evolution of microstructure and fracture behavior of multilayered copper sheet fabricated by accumulative roll bonding. Journal of Materials Research and Technology. 2021;10:291-305.
38. Noor SV, Eivani AR, Jafarian HR, Mirzaei M. Inhomogeneity in microstructure and mechanical properties during twist extrusion. Materials Science and Engineering: A. 2016;652:186-91.